4-1-1998

Experimental results in robust lateral control of highway vehicles

Chaouki T. Abdallah

Raymond H. Byrne

Peter Dorato

Recommended Citation

Abdallah, Chaouki T.; Raymond H. Byrne; and Peter Dorato. "Experimental results in robust lateral control of highway vehicles." *IEEE Control Systems Magazine* 18, 2 (1998): 70-76. doi:10.1109/37.664657.

Experimental Results in Robust Lateral Control of Highway Vehicles

Raymond H. Byrne, Chaouki T. Abdallah, and Peter Dorato

Vehicle lateral dynamics are affected by vehicle mass, longitudinal velocity, vehicle inertia, and the cornering stiffness of the tires. All of these parameters are subject to variation, even over the course of a single trip. Therefore, a practical lateral control system must guarantee stability, and hopefully ride comfort, over a wide range of parameter changes. This article describes a robust controller that theoretically guarantees stability over a wide range of parameter changes. The performance of the robust controller is then evaluated in simulation as well as on a test vehicle. Test results for experiments conducted on an instrumented track are presented, comparing the robust controller to a PID controller that was tuned on the vehicle.

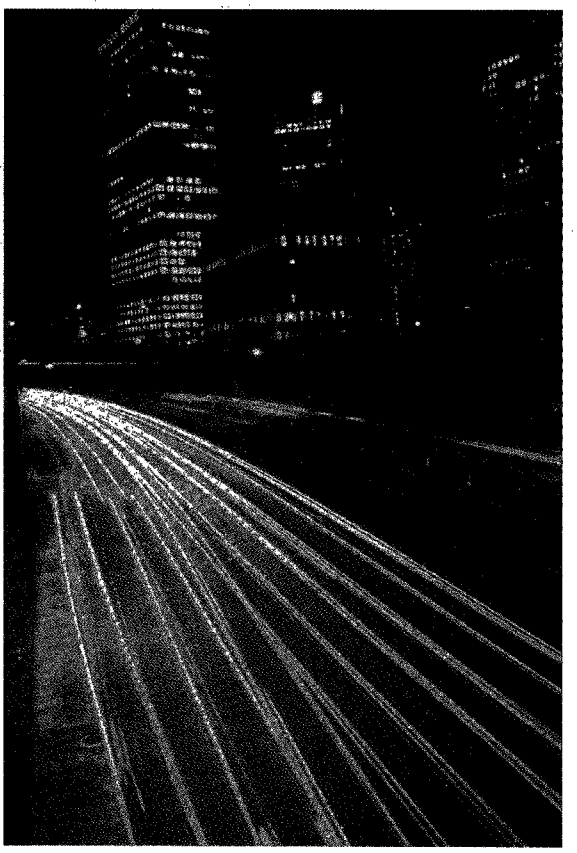

Introduction

One of the fundamental goals of the Intelligent Transportation Systems (ITS) community is to develop automated highways where vehicles are capable of automatically driving down the road, either individually or in platoons of multiple vehicles. In order to implement such a system, a controller that can keep the vehicle centered in the lane is required. There are many factors that make automatic lateral control of vehicles difficult. These include changing vehicle parameters (tire pressure, tire wear, etc.), changing road conditions (rain, ice, bumps, crowns, etc.), as well as disturbances caused by wind and other factors. Another important consideration is driver comfort while performing lane changes and reacting to disturbances.

Initial research efforts on automated highway systems (AHS) were conducted by the Radio Corporation of America in cooperation with General Motors in the late 1950s [1]. A significant amount of research, including the development of prototype experimental equipment, was conducted at The Ohio State University between 1964-1980 [2]. This included research on both lateral and longitudinal control of highway vehicles. The largest current advanced vehicle control system (AVCS) research effort is being conducted at California PATH (Partners for Advanced Transit and Highways) [3-13].

The PATH program has been investigating a frequency shaped linear quadratic (FSLQ) optimal control approach for the lateral controller, with feedforward preview control to reduce feedback gains [3, 5, 6]. Although the FSLQ approach incorporates ride qualities into the performance index, other work that attempts to design a lateral controller taking into account ride comfort is described in [14]. Recent work on robust control applied to car steering is described in [15-22]. While many of the previously mentioned efforts rely on buried magnets, electrified wires, or a microwave radar to determine the vehicle's lateral position, another promising approach involves using vision. Efforts at Carnegie Mellon University (CMU), at the National Institute of Standards and Technology (NIST), and in Germany have yielded promising experimental results using neural networks and classical vision algorithms [23, 24].

This article describes a robust lateral controller that theoretically guarantees stability over a wide range of parameter changes. The controller is designed with the plant uncertainty modeled as unstructured additive perturbations in the frequency-domain. This approach, first described in [25], is reviewed in the next section. Extensions to the current theory that are applied to the car problem are also described in the next section. The modeling of the vehicle's lateral dynamics is discussed in third section. The controller design and

Raymond Byrne is a senior member of the technical staff at Sandia National Laboratories, Albuquerque, NM. Email: [illegible] Chaouki Abdallah and Peter Dorato are with the Electrical and Computer Engineering Department at the Univeristy [illegible] querque, NM. *This work was supported by the United States Department of Energy under contract DE-AC04-94AL850[illegible] tional Lab's Doctoral Study Program.*

 0272-1708/97/$10.00©1997IEEE

simulation results are presented in the fourth section, and experimental test results are presented in the fifth section. A summary and discussion of planned future research is outlined at the end of the article.

The Robust Stability Condition

Modeling system uncertainty as unstructured additive perturbations in the frequency-domain is described by Equation (1), where the nominal plant transfer function is $p_0(s)$, and the uncertainty in the transfer function is $\delta p(s)$.

$$p(s) = p_0(s) + \delta p(s) \tag{1}$$

Using this model for the parameter uncertainty, the following class of systems can be defined.

Definition A.1 [25]: A transfer function $p(s)$ is said to be in the class $C(p_0(s), r(s))$ if

1. $p(s)$ has the same number of unstable poles as that of $p_0(s)$
2. $|p(jw) - p_0(jw)| \le |r(jw)|, |r(jw)| > 0, \forall w \in \mathbb{R}$
3. $r(s)$ is a stable minimum phase transfer function

A robust stabilizer $c(s)$ for $C(p_0(s), r(s))$ stabilizes the closed-loop system for each $p(s) \in C(p_0(s), r(s))$. From [25], $c(s)$ is a robust stabilizer if and only if the nominal closed-loop system is stable, and

$$\left| \frac{r(jw)c(jw)}{1 + p_0(jw)c(jw)} \right| < 1 \forall w \in \mathbb{R} \tag{2}$$

The robust stability condition can be written as

$$\|u(s)\|_\infty < 1 \tag{3}$$

where $u(s)$ satisfies the following interpolation conditions

$$u(\alpha_i) = \tilde{q}(\alpha_i) r_m(\alpha_i) = \frac{r_m(\alpha_i)}{\tilde{p}_0(\alpha_i)} \tag{4}$$

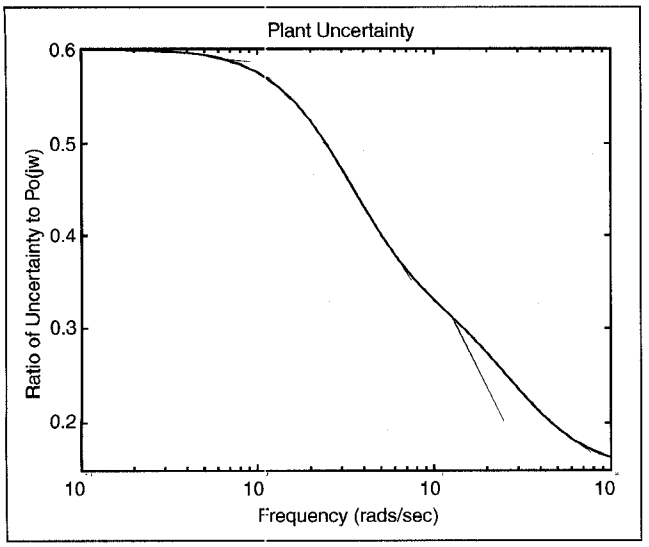

Fig. 1. Simulation of plant uncertainty.

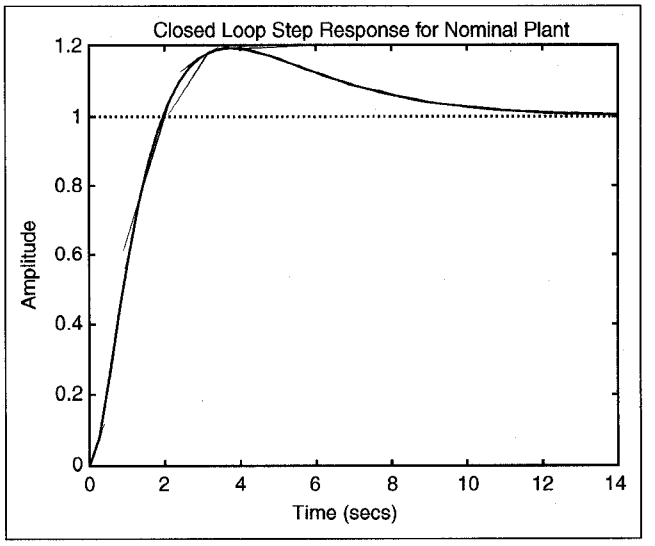

Fig. 2. Step response of closed-loop system with the nominal plant.

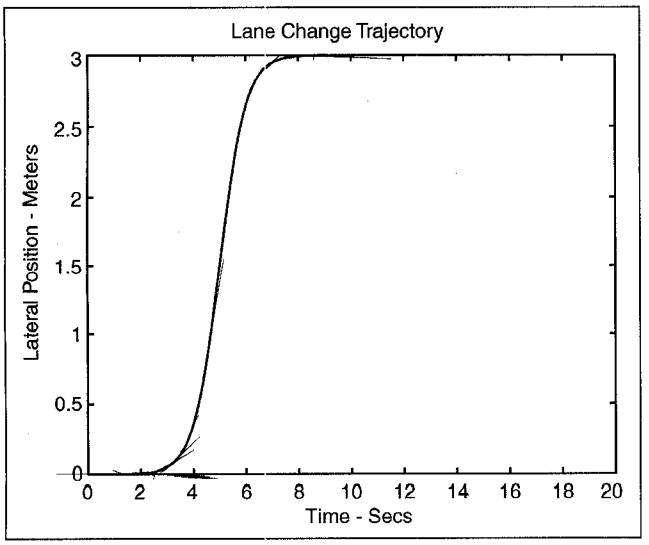

Fig. 3. Lane change trajectory.

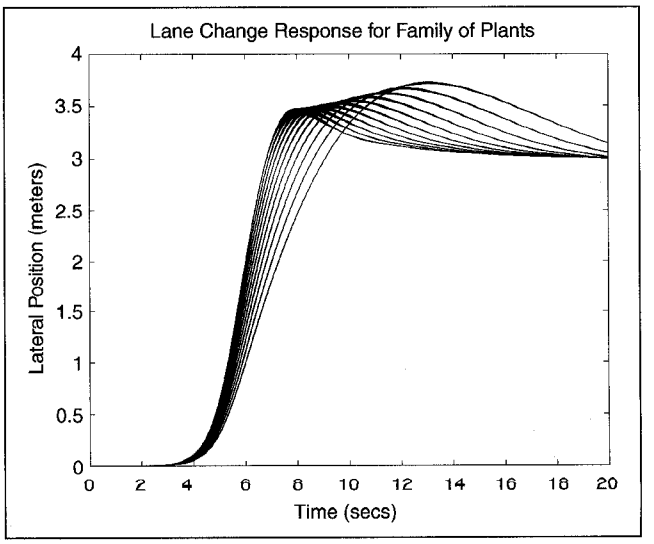

Fig. 4. Lane change response, family of plants.

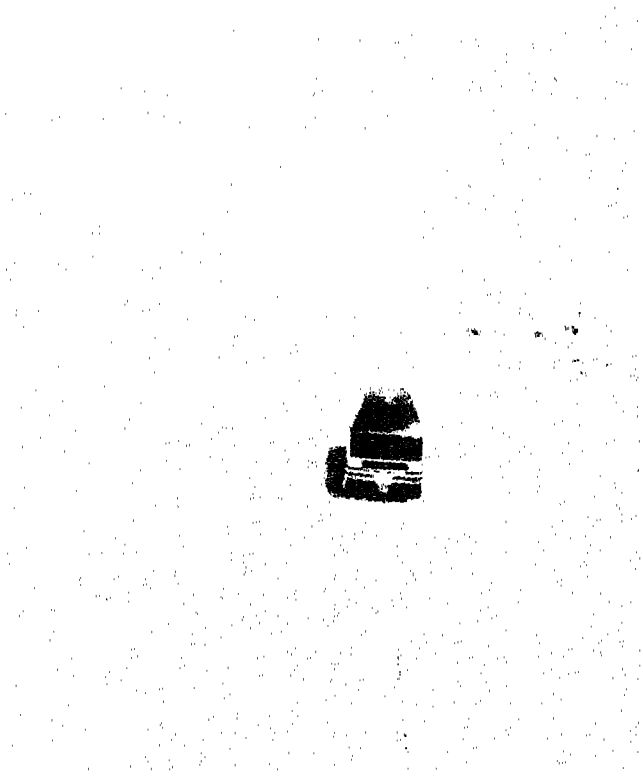

Fig. 5. Photograph of the test vehicle.

where α_i are the poles of the nominal plant in the RHP, $\tilde{p}_0(s)$ is the nominal plant multiplied by a Blaschke product, $\tilde{q}(s)$ is the q parameter divided by a Blaschke product, and $r_m(s)$ is a minimum phase H^∞ function that satisfies $|r_m(jw)| = |r(jw)|$. Constraints are also placed on the relative degree of $u(s)$, depending on the relative degree of $r_m(s)$.

The robust stability problem for additive unstructured perturbations then reduces to the problem of finding a strictly bounded real (SBR) function $u(s)$ that interpolates at the unstable poles of the nominal plant in the RHP. This interpolation problem is often referred to as the Nevanlinna-Pick interpolation problem. There are limitations to the approach presented by Kimura, which arise from limitations of the Nevanlinna-Pick interpolation theory. The current theory has difficulties with interpolation points with multiplicity, as well as with interpolation points on the jw axis. Techniques for handling these two cases are outlined in [26].

For plants with a multiplicity of unstable poles, additional interpolation conditions are placed on $u(s)$. These interpolation conditions are derived in [26], and presented in Equation (5).

$$\left.\frac{d^i}{ds^i}\left[u(s)\right]\right|_{s=\alpha_i} = \left.\frac{d^i}{ds^i}\left[\frac{r_m(s)}{\tilde{p}_0(s)}\right]\right|_{s=\alpha_i} \quad \text{where } i = 1,2,3,\ldots,(m-1) \tag{5}$$

By using a modified Fenyves Array, and a modified mapping, the interpolation conditions described by Equation (5) can be met provided a solution exists [26], even if the interpolation points are on the jw axis. These techniques are applicable to the lateral control of automobiles because the lateral dynamics model contains a double integrator as described in the next section.

Model of Lateral Dynamics

The two-degree-of-freedom linearized bicycle model for a vehicle's lateral dynamics will be used in this section to model the test vehicle, a GMC Jimmy. A detailed description of the linearized bicycle model may be found in [27]. The estimated nominal parameters for the Jimmy and the expected range of values are listed in Table 1. The nominal speed of 8 m/s corresponds to 28.8 kmph, while the extreme speeds correspond to 18 kmph and 36 kmph respectively. These values were chosen because the initial field testing will be conducted at relatively low speeds. Simulation results for highway speeds appear in [28].

Using the values in Table 1, the nominal car model is given by Equation (6).

$$\frac{E_f(s)}{\delta_f(s)} = \frac{114.2552\left(s^2 + 13.4391s + 31.4366\right)}{s^2\left(s^2 + 24.3156s + 151.9179\right)} \tag{6}$$

where E_f is the lateral error (m) at the sensor, and δ_f is the front steering angle (rad)

A MATLAB program was written to determine the bound on the frequency-domain uncertainty of the nominal plant as the velocity and cornering stiffness vary over the ranges in Table 1. The program finds the magnitude of

$$|\delta p(jw)| = |p_0(jw) - p(jw)| \tag{7}$$

where $p_0(s)$ is the transfer function of the nominal plant and $p(s)$ is the transfer function of the actual plant as the parameters are varied. The results of the computer simulation are shown in Fig.

Table 1. Estimated Parameters for S-15 Blazer

Parameter	Description	Nominal Value	Range
m	Vehicle mass	1590 kg	constant
V_x	Longitudinal velocity	8 m/s (28.8 kmph)	5-10 m/s (18-36 kmph)
l_1, l_2	Dist. from axles to c.g.	1.17 m, 1.42 m	constant
C_r, C_f	Tire cornering stiffness	42000 Kn/rad	0.85 to 1.15
I_z	Inertia about z axis	3200 kg · m^2	constant
l^*	Dist. from c.g. to sensor	2 m	constant

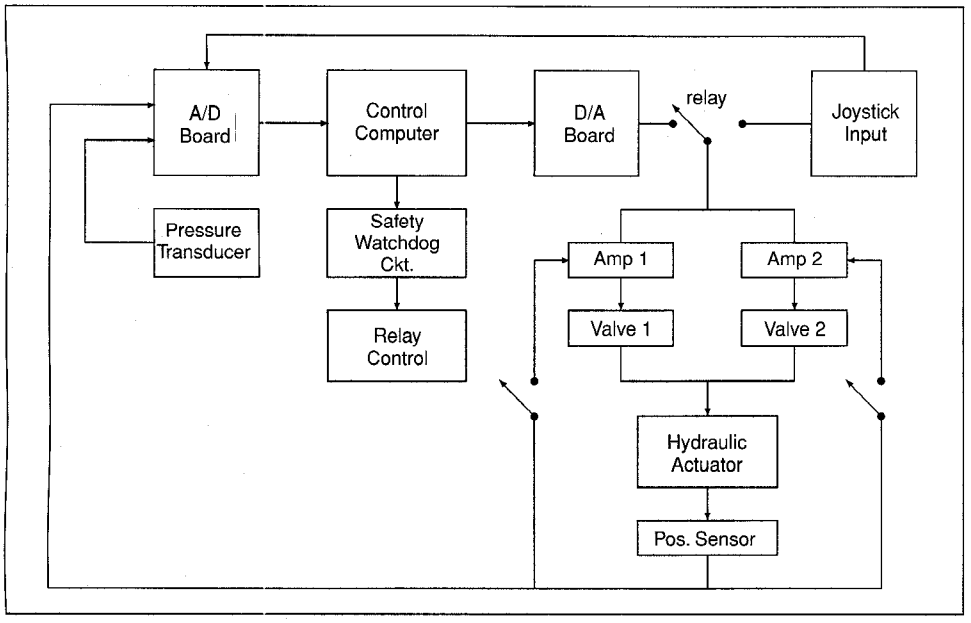

Fig. 6. Block diagram of computer control system.

1. The results are plotted as the ratio $\left|\frac{\delta p(jw)}{p_0(jw)}\right|$. This format of data presentation was chosen because it facilitates the choice of $r(s)$ as a function of $p_0(s)$. This simplifies the calculations required to arrive at the robust controller in the next section.

Controller Design

Using the data in Fig. 1, a conservative bound on the plant uncertainty can be expressed as

$$r(s) = 0.6p_0(s) \tag{8}$$

With this bound, a robustly stabilizing controller can be designed if there exists an SBR solution to the interpolation problem. It should be noted that this choice of uncertainty is equivalent to the uncertain gain problem, whose solution is described in [29, 30]. However, a less conservative gain could be chosen which would require the use of the techniques described in [26].

The nominal plant described by Equation (6) has two poles at the origin and a relative degree of 2. Therefore, the uncertainty bound also has a relative degree of 2. The two poles at the origin can be handled by using the techniques outlined in [26]. The two interpolation points at infinity must be handled differently. One interpolation point at infinity will be handled using the approach described in [25]. The second interpolation point at infinity will be added using Equation (9).

$$u^*(s) = u(s)\Omega(s) \tag{9}$$

By properly choosing $\Omega(s)$, the second interpolation point at infinity can be achieved, while still keeping $u^*(s)$ SBR. An alternate method to handle the multiple interpolation points at infinity would be to map the problem to the z-domain where zeros at infinity are represented as $z = 1$.

A robustly stabilizing compensator for the lateral control problem was obtained in [26] and is shown in Equation (10).

$$c(s) = \frac{(2s^2 + 1.5s + 0.25)(s^2 + 24.3156s + 151.9179)}{114.2552(0.64s^2 + 2.64s + 1.16)(s^2 + 13.4391s + 31.4366)} \tag{10}$$

The poles of the nominal-closed loop system are -2.5, -0.625, and -0.5. These are the poles of $u^*(s)$. The step response of the closed-loop system is shown in Fig. 2.

The lane change trajectory shown in Fig. 3 was used to simulate the family of plants as the cornering stiffness and velocity

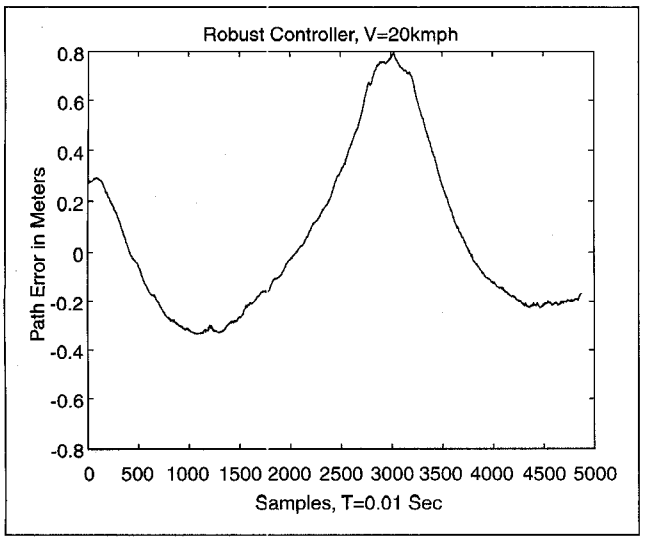

Fig. 7. Robust controller, V_x = 20 kmph.

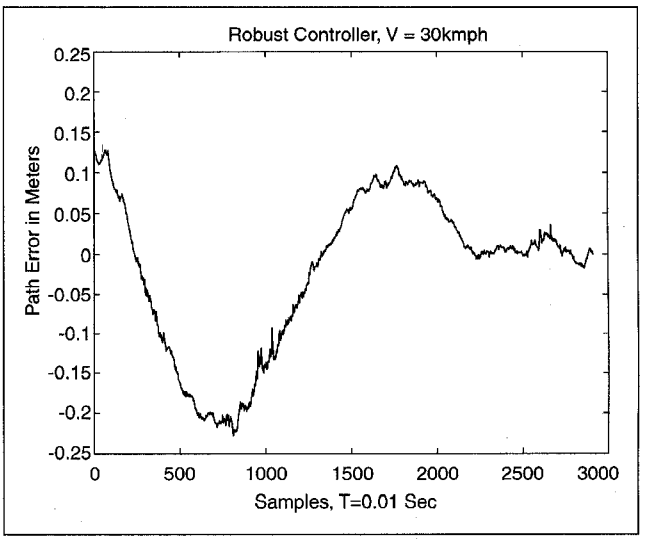

Fig. 8. Robust controller, V_x = 30 kmph.

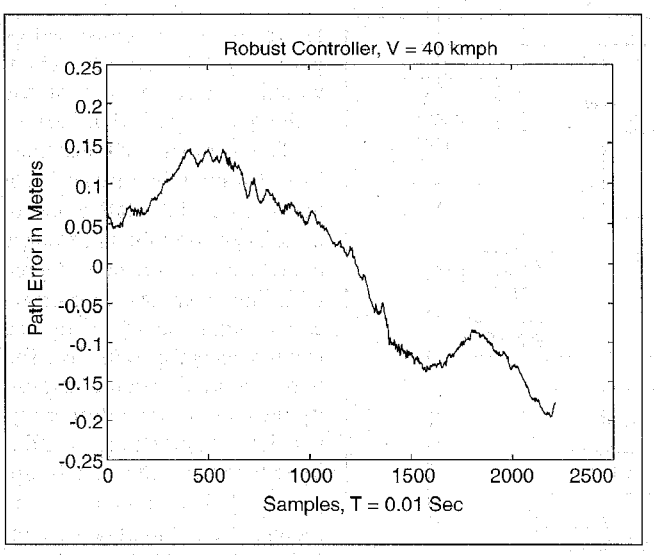

Fig. 9. Robust controller, $V_x = 40$ kmph.

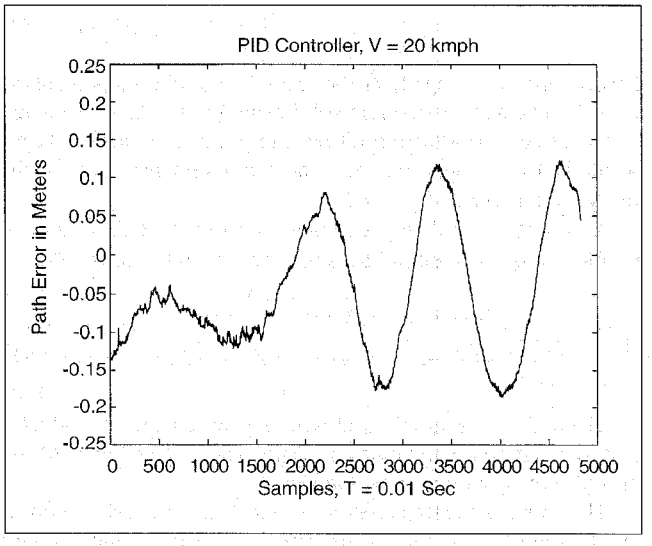

Fig. 10. PID controller, $V_x = 20$ kmph.

were varied. The lane change performance of the family of plants is shown in Fig. 4. The lane change response for the family of plants varies as the model changes, but all responses are stable and slightly underdamped. The maximum percent overshoot is approximately 20 percent. Modifications in the response of the system may be made by choosing a different function for the last row of the Fenyves Array (similar to U-parameterization [31]), and by choosing a different ε in the modified mapping (see [26]). Test results for the robust lateral control algorithm are presented in the next section.

Table 2. RMS Error for PID and Robust Controllers

Speed (kmph)	Robust Controller rms error	PID Controller rms error
20	0.1085 m	0.0857 m
30	0.0751 m	0.0858 m
40	0.0953 m	0.0779 m

Test Vehicle

The theoretical lateral control algorithm presented in the previous section was implemented on a test vehicle, shown in Fig. 5. For the purposes of this research, the 1989 GMC Jimmy was modified for drive-by-wire operation, where there are no mechanical linkages between the driver's steering commands and the motion of the wheels. Under manual operation, the driver provides steering commands with a joystick mounted between the two front seats. Under automatic operation, the control computer provides steering commands to keep the vehicle centered in the lane. In both cases, the control computer is responsible for maintaining the desired steering angle. A linear hydraulic actuator connected to the tie-rod provides steering actuation. Steering angle and actuator position were sensed with a linear potentiometer in parallel with the linear actuator. A back-up analog steering control system was activated by a safety watchdog circuit to ensure safe operation in the event of a computer failure. The analog system was activated if the steering servo loop failed to execute within a preset time interval.

The power steering pump was modified to charge a large hydraulic accumulator, which stores enough hydraulic fluid under pressure to provide 30 lock-to-lock steering maneuvers in the event of a pump failure. A pressure sensor sounds an alarm if the hydraulic system pressure drops below a specified value—alerting the driver to stop operation of the test vehicle. The hydraulic system was also designed with two redundant valves so that a valve failure would not result in a loss of steering control. By having two valves in parallel, a failure of one valve will reduce the maximum flow rate, but will still allow the automatic steering system to function. In addition, low-cost proportional solenoid valves were used instead of high-performance servo valves. Proportional solenoid valves have a bandwith of approximately 20 Hz, compared to 100 Hz for servo valves. A block diagram of the computer control system is shown in Fig. 6.

A one-mile test track was instrumented with a wire reference system to sense the lateral position of the vehicle. The wire loop was driven with a 9.6 KHz, 24-volt square wave signal. The drive electronics consisted of a crystal oscillator, a divide-by-N counter circuit, and a power mosfet. The sensing circuit on the vehicle consisted of a tuned LC-circuit, with a sensor located on the left and right bumper. The raw sensor data at each bumper was processed with analog electronics to generate an error signal proportional to the lateral position error of the vehicle.

Test Results

The lateral control algorithm presented in the previous section was discretized using the bilinear transformation

$$s = \frac{2}{T}\frac{z-1}{z+1}, T = 100 \text{ ms} \tag{11}$$

with a sampling period of 100 ms. The gain of the theoretical controller was increased by a factor of two to overcome approximately one degree of backlash in the steering actuator. A small integration term was also added to the robust controller to overcome center steering offsets and road superelevation. Testing was conducted on a straight section of the track, at speeds of 20 kmph, 30 kmph, and 40 kmph.

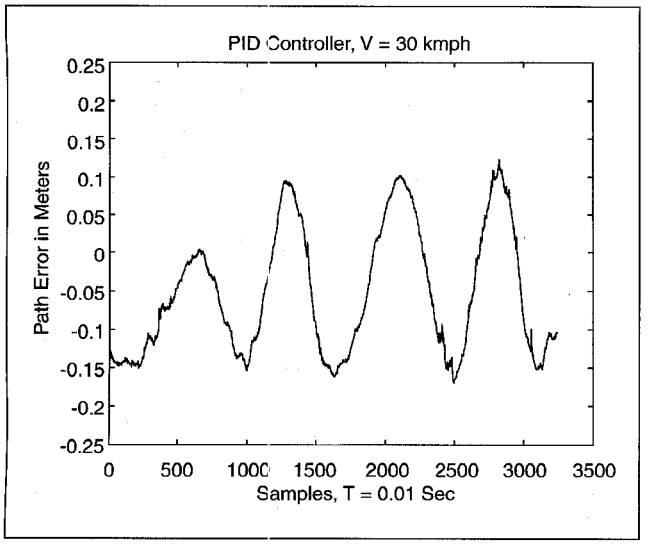

Fig. 11. PID controller, V_x = 30 kmph.

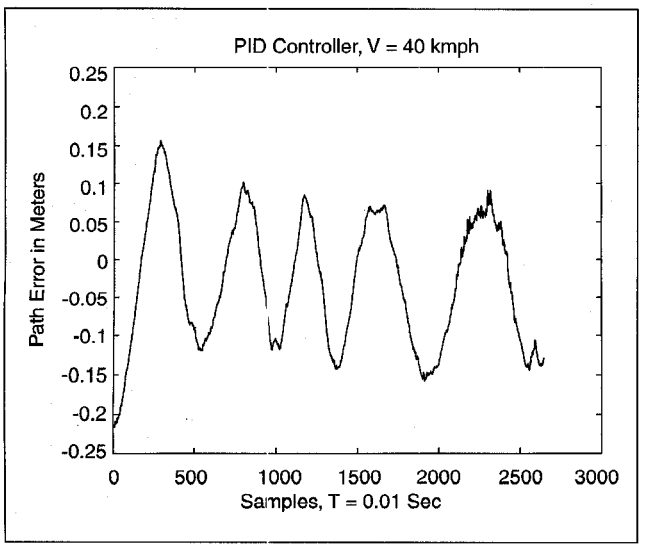

Fig. 12. PID controller, V_x = 40 kmph.

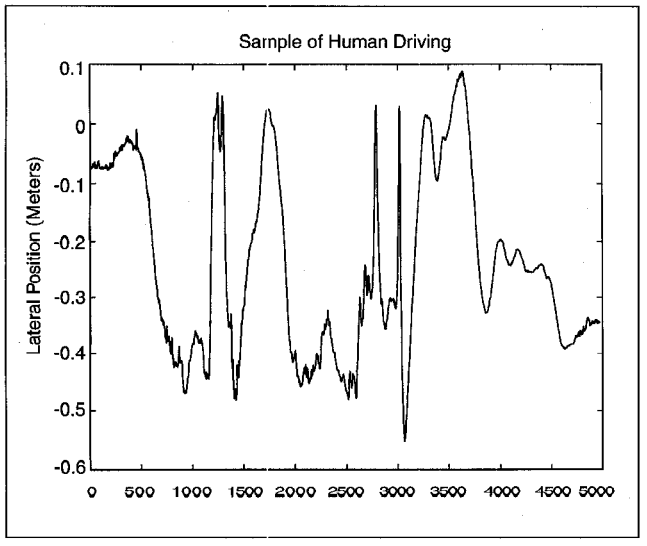

Fig. 13. Human driving sample.

Because of the fixed test distance, slower speed runs produced more data than higher speed runs. The test results are shown in Figs. 7-9.

A proportional-integral-derivative (PID) control algorithm was also implemented for comparison to the robust controller. The gains of the PID controller were hand-tuned on the vehicle. Tuning the PID controller on the vehicle presented some difficulties. Gain values accidentally set too high yielded unstable behavior, which resulted in a very rough ride. The performance of the PID algorithm at the same three speeds is shown in Figs. 10-12. A summary of the rms error for each test run appears in Table 2.

Looking at the test results, and at the rms error summarized in Table 2, both controllers performed satisfactorily at the speeds tested. To allow a fair comparison of the automatic controllers, a sample of human driving is provided in Fig. 13. This data was taken as the speed varied between 30 kmph and 60 kmph. The human driving sample shows that the performance of the automatic control systems is equal to or better than the human driving. It should be noted that the performance measurement, rms error, was not incorporated into the controller design (robust or PID). However, it is customary to speak about the rms error (or maximum error), when discussing test results.

The rms error for the PID controller is better at 20 kmph and 40 kmph. The nominal plant for the robust control design was at 28.8 kmph, so it would seem reasonable that the best performance of the robust controller would be at 30 kmph. At this speed, the performance of the robust controller was slightly better than the PID controller. There are several difficulties with the robust controller implementation, however. The robust controller was very sensitive to the accuracy of the center steering position as well as to the initial orientation of the vehicle. The test data presented for the robust controller was obtained with the vehicle starting centered and headed in the proper direction. If the vehicle was started in a different orientation, headed slightly to the left or right, the robust controller had difficulty correcting. In addition, adding an offset to the center steering position will cause the robust controller to have difficulty keeping the vehicle centered in the lane. Both of these difficulties represent unmodeled dynamics that were not taken into account in the robust controller design and uncertainty modeling. Therefore, it is reasonable that the robust controller should have difficulty with these conditions, even with the addition of a small integration term.

Comparing the robust controller to the PID controller, the robust controller results in fewer oscillations. The performance of the PID controller could almost be described as steady state, slow oscillation. The period of the oscillations is very large, and is almost imperceptible by the driver. The higher gain and integration term in the PID controller contribute to the oscillations, but also help the controller overcome some of the unmodeled disturbances like steering angle offsets and actuator backlash. Because of this, the PID controller is able to handle deviations in initial orientation much better than the robust controller. The PID controller also operates successfully up to 60 kmph, while the maximum speed of the robust controller is approximately 40 kmph. One of the most useful results of the hardware implementation is the identification of steering actuator backlash, center steering offsets, and road disturbances as problematic areas for control system implementation. These items, in addition to parameter variations, must also be considered when designing a truly robust control system.

Summary and Conclusions

This article presents experimental results for a robust lateral control system designed for an automated vehicle. The benefits of a robust control algorithm include guaranteed stability over a wide range of operating conditions and a fixed controller as opposed to gain scheduling. For this application, the uncertainty in vehicle velocity and cornering stiffness were modeled as unstructured additive perturbations in the frequency-domain. Based on the expected uncertainty modeling, interpolation techniques described in [26] were used to design a robust lateral control algorithm. The robust controller was then tested on a GMC Jimmy test vehicle that was modified for drive-by-wire operation. Testing was conducted on straight sections of an instrumented one-mile test track. A PID controller that was tuned on the vehicle was also implemented for comparison purposes.

Although the robust controller performed satisfactorily, the vehicle control experiments highlighted several implementation difficulties. The uncertainty modeling was fairly conservative, which resulted in a performance trade-off. Unmodeled uncertainties like steering actuator backlash and center steering offsets were also problematic. In addition, the robust controller was sensitive to initial vehicle orientation at the start of the test runs. Future research will focus on incorporating these types of uncertainty into the controller design as more structured uncertainty. By incorporating more knowledge of the system uncertainty into the robust design, performance can probably be improved while still maintaining the desired robustness to parameter changes. Since the car model is minimum phase, we have explored using the simultaneous stabilization approach developed by Barmish and Wei [32]. This approach has been implemented in simulation, but has not been used on the test vehicle.

Raymond Byrne is a senior member of the technical staff at Sandia National Laboratories in Albuquerque, N.M., where he has been employed for the last eight years. He received a B.S.E.E. from the University of Virginia in 1987, an M.S.E.E. degree from the University of Colorado (Boulder) in 1989, and a Ph.D. in electrical engineering from the University of New Mexico in 1995. He is a member of IEEE, Tau Beta Pi, Eta Kappa Nu, and Sigma Xi. His research interests include autonomous and teleoperated mobile robots, control architectures for large numbers of robots, and control system implementations.

Chaouki Abdallah received his B.E. degree in electrical engineering in 1981 from Youngstown State University, Youngstown, Ohio, his M.S. degree in 1982 and the Ph.D. in electrical engineering in 1988 from Georgia Tech, Atlanta, Georgia. Between 1983 and 1985 he was with SAWTEK Inc., Orlando, Fla. He joined the department of electrical and computer engineering at the University of New Mexico, Albuquerque, N.M., in 1988 and was promoted to associate professor in August 1994. Dr. Abdallah was exhibit chairman of the 1990 International Conference on Acoustics, Speech, and Signal Processing (ICASSP) and is currently serving as the local arrangements chairman for the 1997 American Control Conference. His research interests are in the areas of robust control, adaptive and nonlinear systems, and robotics. Dr. Abdallah is a senior member of IEEE. He is a co-editor of the IEEE press book titled *Robot Control: Dynamics, Motion Planning, and Analysis*, and co-author of a book titled *Control of Robot Manipulators*, published by Macmillan, and another titled *Linear Quadratic Control: an Introduction*, published by Prentice Hall.

Peter Dorato is a professor of electrical and computer engineering at the University of New Mexico. He received the B.S.E.E. from the City College of New York, M.S.E.E. degree from Columbia University, and the D.E.E. degree from the Polytechnic Institute of Brooklyn (now the Polytechnic University). He has been a faculty member at the Polytechnic University and the University of Colorado at Colorado Springs, and from 1976 to 1984 he was chairman of the electrical and computer engineering department at the University of New Mexico. He was a visiting professor at the University of California at Santa Barbara during the academic year 1984-1985, and at the Politecnico di Torino, Italy, during the academic year 1991-1992. His current areas of interest include multivariable systems, robust control, optimal control, and engineering education. He is a fellow of IEEE, Distinguished Member of the IEEE Control Systems Society, and a registered professional engineer (in the state of Colorado). He is currently editor of the technical communiques for *Automatica*, and is a past associate editor of the *IEEE Transactions on Automatic Control*. He edited three IEEE Press reprint volumes, *Robust Control*, *Recent Advances in Robust Control*, and *Advances in Adaptive Control*, and is the co-author of two books, *Robust Control for Unstructured Perturbations: An Introduction* and *Linear Quadratic Control: An Introduction*.